GeV Electrons via Laser Wakefield Acceleration with Pre-formed Plasma Channels

Nathaniel Tamminga

Candidacy Written Exam

Department of Physics

The Ohio State University

ADVISOR

Dr. Chris Orban

COMMITTEE

Dr. Doug Schumacher

Dr. Enam Chowdhury

Dr. Greg Kilcup

August 18, 2023

CONTENTS

LIST OF FIGURES

I. INTRODUCTION

The idea of laser-driven plasma-based electron accelerators was originally envisioned in 1979 by Tajima and Dawson [7]. Since then, laser-plasma accelerators have made great strides in their practicality and are gaining interest for a variety of applications due to their small size and large electric fields. These applications include free-electron lasers, Thomson sources, and a variety of different high energy particle colliders [8]. In order to make these different applications a reality, electron beams with energies of 10 GeV and a low beam energy RMS are required. These energies are becoming more of a reality, since over the past decade, beam energies have grown from 0.5 GeV to 8 GeV [8, 9].

These advancements have come from improvements in plasma waveguide technology. The two most prominent waveguide methods in the gas targets we are dealing with are capillary discharge and optical field ionization (OFI). The principles behind the plasma waveguides are similar, but the manner in which the waveguides are formed differs. To understand how these waveguides work and why they lead to higher electron beam energies, we must first look at the method in which these electron beams are accelerated, mainly laser wakefield accelerators (LWFA).

II. LASER WAKEFIELD ACCELERATORS

A. Physics of LWFA

Laser wakefield acceleration (LWFA) is a method of accelerating electrons in a plasma. In this process, electrons are accelerated by large electric field gradients in the wakefield. This process occurs when a single, short, high-intensity laser pulse drives a plasma wave in an underdense plasma. In this regime, short is $t \leq 1ps$, high-intensity is $I \geq 10^{17} W/cm^2$, and underdense is $(\omega/\omega_p)^2 \gg 1$. ω_p is the electron plasma frequency, $\omega_p = \sqrt{\frac{n_0 e^2}{m_e \epsilon_0}}$. n_0 is the ambient electron number density, e is the electron charge, and m_e is the rest mass of an electron and ϵ_0 is the permittivity of free space [2]. Due to the short pulse requirements, LWFA did not become a viable application until the development of femtosecond lasers in the 1980s.

As the laser pulse propagates through a plasma, the ponderomotive force of the laser

vacates electrons from the laser region. The ponderomotive force is given by equation II.1.

$$\vec{F_p} = -\frac{e^2}{4m\omega^2}\vec{\nabla}(E^2) \tag{II.1}$$

Where e is the elementary charge, m is the rest mass of an electron, ω is the frequency of the incoming laser pulse, and E is the electric field of the laser. This force can be derived from the Lorentz force equation for a charged particle in an electromagnetic field. The ponderomotive force comes from the case where there is an inhomogeneous field which causes the particle to be expelled from the region of the laser pulse.

From this equation, it is seen that a particle will be accelerated towards regions of weaker electric field, effectively clearing out electrons from the region of the laser. For example, if there is a linearly polarized Guassian laser pulse propagating through a plasma, near the peak focus the electric field will have the form of II.2 where r is the radial distance from the beam axis (x and y if the beam is propagating in the z direction), t is the time variable and τ is some time constant.

$$\vec{E}(\vec{r}, t) \propto e^{-r^2/\sigma^2} e^{-t^2/\tau^2} \tag{II.2}$$

Assume the wave is traveling near the speed of light, so at the moment that the peak intensity has reached the origin ($z = 0$), one can substitute $t = z/c$. This will give a picture of what the electric field looks like spatially at that moment.

$$\vec{E}(\vec{r}, t) \propto e^{-\left(x^2+y^2\right)/\sigma^2} e^{-z^2/c^2\tau^2} \tag{II.3}$$

Where in the above, r^2 can be expressed as $r^2 = x^2 + y^2$. This beam will produce a ponderomotive force proportional to II.4.

$$\vec{F_p} \propto -\vec{\nabla}\left(e^{-\left(x^2+y^2\right)/\sigma^2} e^{-z^2/c^2\tau^2}\right)^2 = \left(\frac{4x}{\sigma^2}\hat{x} + \frac{4y}{\sigma^2}\hat{y} + \frac{4z}{c^2\tau^2}\hat{z}\right) e^{-2\left(x^2+y^2\right)/\sigma^2} e^{-2z^2/c^2\tau^2} \tag{II.4}$$

This force will initially push the particle out from the laser field because of the positive linear terms. However, eventually, the exponential decay will bring the force back down to 0. This means that after the electron has left the beam spot, the laser will no longer apply a force to it.

The depletion of electrons by the ponderomotive force of the laser creates a volume, or

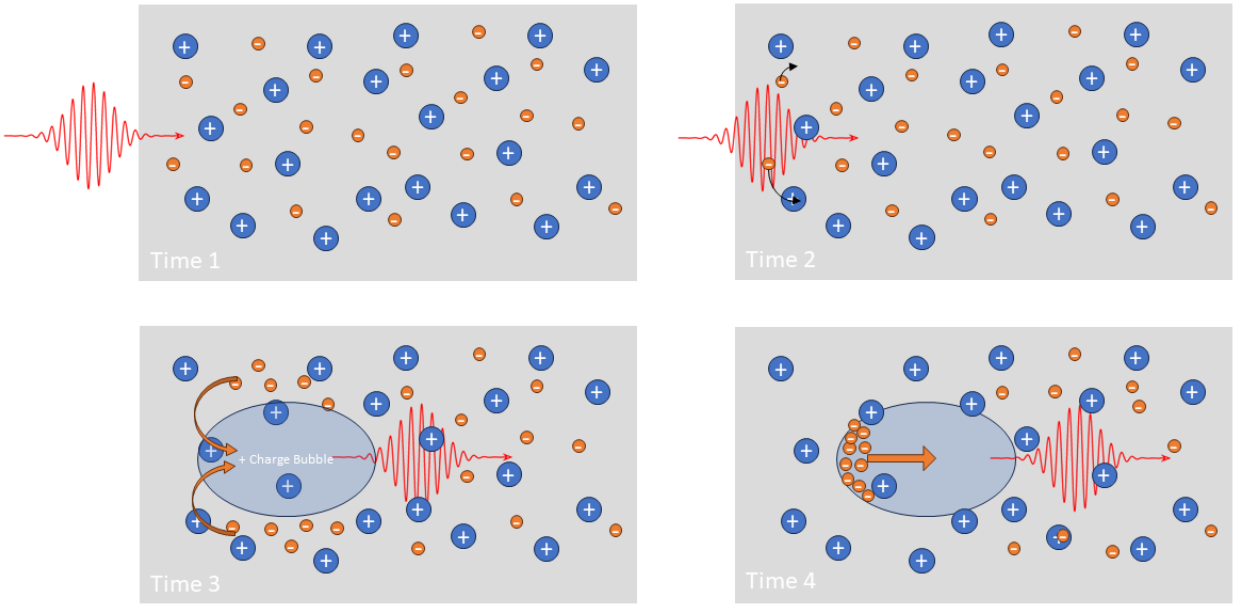

FIG. 1. Illustration of the ponderomotive force vacating electrons as the laser pulse passes through the plasma and creates a plasma wave.

"bubble", of net positive charge immediately behind the laser pulse. This volume is of the order $V = \pi\sigma^2 c\tau$. The electrons are attracted into this region of positive charge immediately following the laser. However, in order for wakefields to form and propagate behind the laser, the laser pulse length needs to be short. If the pulse is too long ($\sigma \ll c\tau$), then the vacated electron channel has a cylindrical shape, and wakefields cannot form and propagate. If the pulse is short ($\sigma \gg c\tau$), then the evacuated region looks more like pancake than a cylinder, which is effective for accelerating electrons. This is why the development of the femtosecond laser pulse was necessary for wakefield acceleration. The femtosecond pulse duration is short enough to allow wakefield propagation. For the best propagation of plasma wakefield waves, the laser pulse length should be $L_t \leq \pi c/\omega_p$, where c is the speed of light in vacuum and ω_p is the plasma frequency [7].

As the electrons are attracted into the area of positive charge, some electrons begin propagating with the wave, being continually attracted to the area of positive charge behind the laser. This is illustrated in FIG. 1. This wave, with peaks and troughs of opposite charge, creates large electric fields over very short distances, > 100 GV/m [2].

Since the bubble is forming at the speed of the laser, the plasma waves travel at the same speed as the laser propagates. This is seen by the fact that the laser group velocity is the

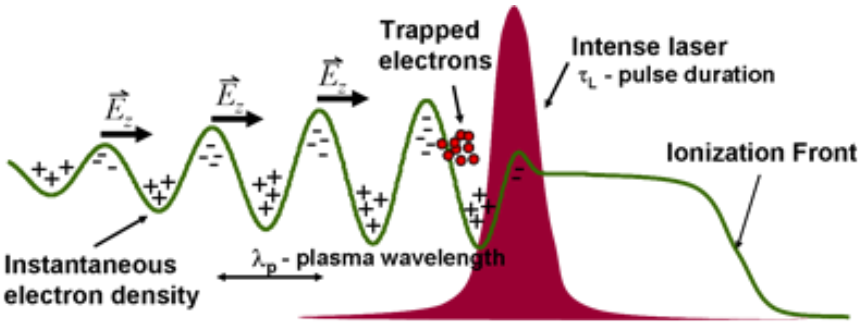

FIG. 2. Illustration of an intense laser pulse interaction with a initially neutral, low number density gas target. Gas is ionized by a heater pulse and the wakefield is created behind the laser. Trapped electrons in the right phase can be accelerated to very high energies. [1]

same as the plasma waves' phase velocity II.5 as shown by Tajima [7].

$$v_p = \frac{\omega_p}{k_p} = v_g^{EM} = c\sqrt{1 - \frac{{\omega_p}^2}{\omega^2}} \tag{II.5}$$

In II.5, v_p is the electron wave phase velocity, k_p is the plasma wave number, v_g^{EM} is the laser group velocity, ω is the angular frequency of the light pulse, c is the speed of light in vacuum, and ω_p is the plasma frequency [2].

These wakefields formed in the plasma create large electric fields as seen in FIG. 2. The wakefield, which travels close to c with low enough electron densities II.5, can trap and accelerate electrons. These electrons are accelerated to highly relativistic speeds, allowing them to stay in phase with the wakefield for a significant distance [7]. This allows electron beams to be accelerated to GeV energies from LWFA.

B. Benefits of Waveguides

Plasma channel guiding works by creating index of refraction gradients. The change in index of refraction leads to total internal reflection, which guides the laser beam through the channel without any deformation to the pulse shape. The index of refraction for a plasma is given as II.6 where ϵ is the dielectric constant II.7.

$$\eta = \sqrt{\epsilon} = \sqrt{1 - \frac{\omega_p^2}{\omega^2}} \tag{II.6}$$

$$\epsilon = 1 - \frac{\omega_p^2}{\omega^2} \tag{II.7}$$

Assume a quadratic electron density like II.8.

$$n_e(r) = n_0 + \Delta n \frac{r^2}{{r_0}^2} \tag{II.8}$$

n_0 is the ambient electron density, $\Delta n = n_e(r_0) - n_e(0)$ is the channel depth, and r_0 is the channel radius. ω_p is the plasma frequency, and ω is the frequency of the light. Substituting in the quadratic electron density into the plasma frequency gives II.9.

$$\omega_p(r) = \sqrt{\frac{[n_0 + \Delta n r^2/{r_0}^2]e^2}{m_e \epsilon_0}} \tag{II.9}$$

$$\omega_{p0} = \sqrt{\frac{n_0 e^2}{m_e \epsilon_0}}$$

An electron density of this form will make the index of refraction II.10.

$$\eta = \sqrt{1 - \frac{\omega_{p0}^2}{\omega^2}\left(1 + \frac{\Delta n}{n_0}\frac{r^2}{r_0^2}\right)} \tag{II.10}$$

If the plasma is underdense ($\frac{\omega_p^2}{\omega^2} \ll 1$), then the first order Taylor expansion can reasonably be taken. The index of refraction will have the form of II.11 [2].

$$\eta(r) \approx 1 - \frac{\omega_{p0}^2}{2\omega^2}\left(1 + \frac{\Delta n}{n_0}\frac{r^2}{{r_0}^2}\right) \tag{II.11}$$

Equation II.8 shows that a minimum electron density is needed on axis, known as the core, while a higher density cylindrical shell is needed around the core, known as the cladding. This leads to a high index of refraction in the core and a lower index of refraction in the cladding. This will produce total internal reflection of the laser as long as the channel depth is the critical channel depth, $\Delta n = \Delta n_c = (\pi r_e {r_0}^2)^{-1}$, and the beam spot size is the same as the channel spot size, $r_s = r_0$ [2]. r_e is the classical electron radius and r_0 is the channel spot size. It is seen in FIG. 3 that the presence of a plasma channel guide greatly improves the distance that a laser pulse can travel while keeping its original beam profile.

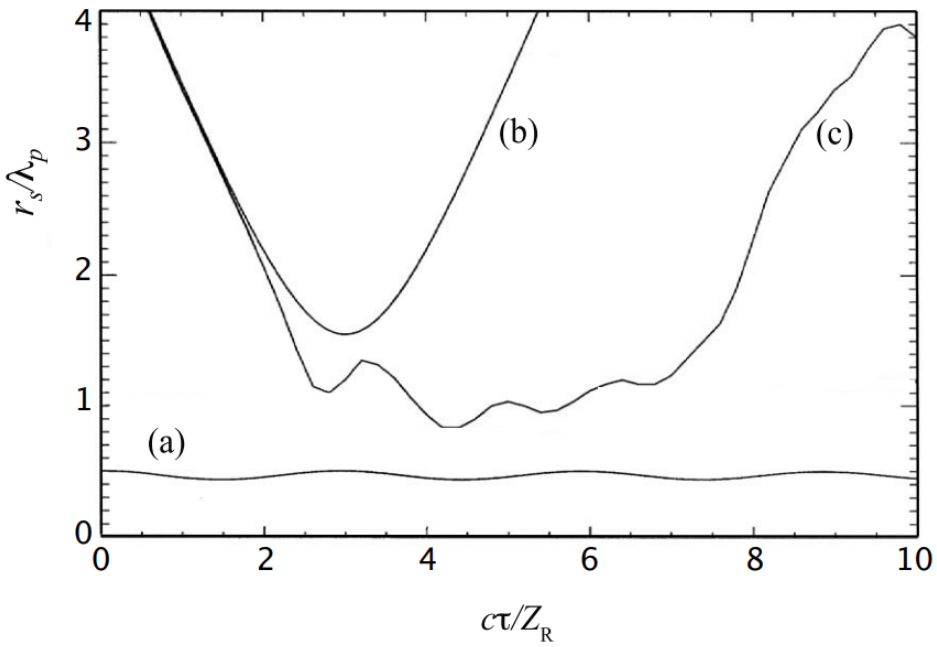

FIG. 3. Laser spot size (r_s) vs propagation distance normalized by Rayleigh length for (a) a channel-guided LWFA, (b) vacuum diffraction, and (c) self-modulated LWFA. From FIG. 28 in [2].

C. Methods of Waveguide Formation

Plasma density channels can be created through several different methods. A single intense laser pulse can create a channel through a combination of ponderomotive force and thermal effects. Channels can also be created through long pulse driven hydrodynamic expansion which varies the radial plasma density profile. However, these two methods are limited by the length of laser propagation in the plasma. This distance is limited to several Rayleigh lengths. The two most promising methods for creating plasma density profiles are short pulse driven hydrodynamic expansion, otherwise known as optical field ionization (OFI), and capillary discharge [2]. These two methods are responsible for producing the highest energy electron beams through LWFA methods. The following paper will discuss how each method works, the history of the work that has lead to our current understanding, the most recent experimental results, and any future work that has been discussed in the field.

Optical Guiding Method	Max Electron Beam Energy	Channel Formation Pulse	Citations
Relativistic Self-Guiding	2 GeV	N/A	[10–13]
Capillary Discharge	4 GeV	N/A	[9, 14, 15]
Discharge + Laser Heating	8 GeV	∼Nanosecond	[8, 16]
OFI	5 GeV	∼Femtosecond	[5]
OFI + 2 Bessel	10 GeV (Simulated)	∼Femtosecond	[6]

TABLE I. A comparison of the most prominent methods of guiding a laser pulse through a plasma along with the electron beam energies they produce and the beam energy spread.

III. RELATIVISTIC SELF-GUIDING

Relativistic self-guiding is an appealing option for propagating lasers long distances because it does not require the production of a pre-formed plasma channel. In relativistic self-guiding, a high power laser beam alters the refractive index through a combination of thermal, ponderomotive, and relativistic effects. This change to the refractive index causes the laser to focus back on axis. At a certain power, the focusing due to alterations of the refractive index will counter the beam diffraction. The power where this happens is called the critical power and is given by III.1 [17].

$$P_{cr} = \frac{m_e^2 c^5 \omega^2}{e^2 \omega_p^2} = 17.4GW(\frac{\omega}{\omega_p})^2 \tag{III.1}$$

If the laser power is greater than the critical power, $P > P_{cr}$, then the laser will begin focusing back towards the axis of propagation. This focusing will cause a higher intensity, further altering the index, and causing more focusing. This effect is known as catastrophic self focusing. Eventually a pulse of critical power will stop propagating because of higher order nonlinear effects, like erosion of the leading edge of the laser pulse.

The critical power can be increased by lowering the plasma frequency, which requires lowering the electron density. However, one cannot simply lower the electron density and expect to get higher electron beam energies. This is because of wave breaking. Wave breaking gives the maximum electric field of an electron wave as III.2 [18].

$$E = \frac{c m_e \omega_p}{e} \tag{III.2}$$

The electric field can be increased, causing greater acceleration over shorter distances, by increasing the plasma wavelength, which requires increasing the electron density. This

places limitations on the effectiveness of relativistic self-guiding. To guide over a 10 cm targert and reach 10 GeV electron beam energies, an electron density of $10^{18} cm^{-3}$ would be needed. This limits the critical power to $P_{cr} = 30TW$.

Electron beam energies of $> 1\ GeV$ have been produced with relativistic self-guiding [13]. This was done at the Callisto laser system at Lawrence Livermore National Lab. In this experiment, a 250TW, 60fs pulse from a Ti:Sapphire laser was focused down to a 15 μm spot radius. This pulse travelled through a 1.3cm gas target made up of 97% He, 3% CO_2 at a density of $1.3 \times 10^{18} cm^{-3}$. This power is about 10 times the critical power for the given target density. However, catastrophic self-focusing did not destroy the laser guiding because the target length was short, only 15 Rayleigh lengths [13]. While relativistic self-guiding can produce GeV electron beams, it is limited by the critical power.

IV. CAPILLARY DISCHARGE

Capillary discharge waveguides work by discharging electrodes across a gas-filled channel. The gas in the channel is ionized through Ohmic heating. The walls of the channel are cooled, leading to a radial temperature gradient. The hot gas in the center of the channel will expand into the cooler gas, creating a density gradient, with a low density core and high density cladding [9]. A schematic of a capillary discharge waveguide is shown in FIG. 4.

The concept of plasma waveguides has been around since the 1990s [19, 20]. However, the idea of using capillary discharge to create a plasma waveguide did not come until the early 2000s [3, 21]. Capillary discharge was first demonstrated as a viable method of producing plasma channels by a team from Oxford, but this experiment did not produce electron beams to due to insufficient laser intensity, $I \leq 10^{17} W cm^{-2}$ and a non-optimized delay between the current discharge and laser pulse arrival [21].

The first demonstration of capillary discharge to produce electron beams was done by a group at Lawrence Berkeley National Lab (LBNL) [9]. In this experiment, several parameters were altered from the Oxford experiment. The initial gas density was decreased to allow maximum laser pulse transmission, the delay between the discharge current and arrival of the laser pulse was optimized, and there was a small increase in intensity, $I = 10^{18}\ W\ cm^{-2}$. A 40 fs FWHM pulse from a Ti:Sapph laser was focused down into a spot with a 25 μm radius. The electrodes discharged $80 - 110\ ns$ prior to the laser pulse arriving. The pulse

then propagated through a 33 mm long channel with a diameter of 190-300 μm and an initial gas density of $3.2 - 4.3 \times 10^{18}\ cm^{-3}$ to produce electron beams with energies of 0.5-1.0 GeV. Ultimately, the beam energies were limited by the laser stability and length of the plasma channel [9].

The same group from LBNL was able to increase the energy of the electron beam from 1.0 GeV to 4.2 GeV through several adjustments [14, 15]. The laser energy was increased from the mJ regime to ≈16J with a beam radius of 52 μm at the focus. The waveguide channel was lengthened from 3.3cm long to 9cm, allowing the electrons to be accelerated to higher energies over longer distances. The channel size was increased to 500μm and the electron density was decreased to $7 \times 10^{17}\ cm^{-3}$. All these changes contributed to the production of a 4.2 GeV electron beam. This experiment had about the same energy spread, 5-6 % rms, compared with the 2006 experiment. It had a much better angular divergence of 0.3mrad compared with a 3mrad divergence in 2006. Electron beam energies were limited by laser pointing instabilities, insufficient density gradients, and short channel lengths. Simulation results [15] predicted electron beam energies of >10 GeV if laser stability and alignment can be improved, steeper density gradients can be formed, and longer plasma channels produced [14, 15].

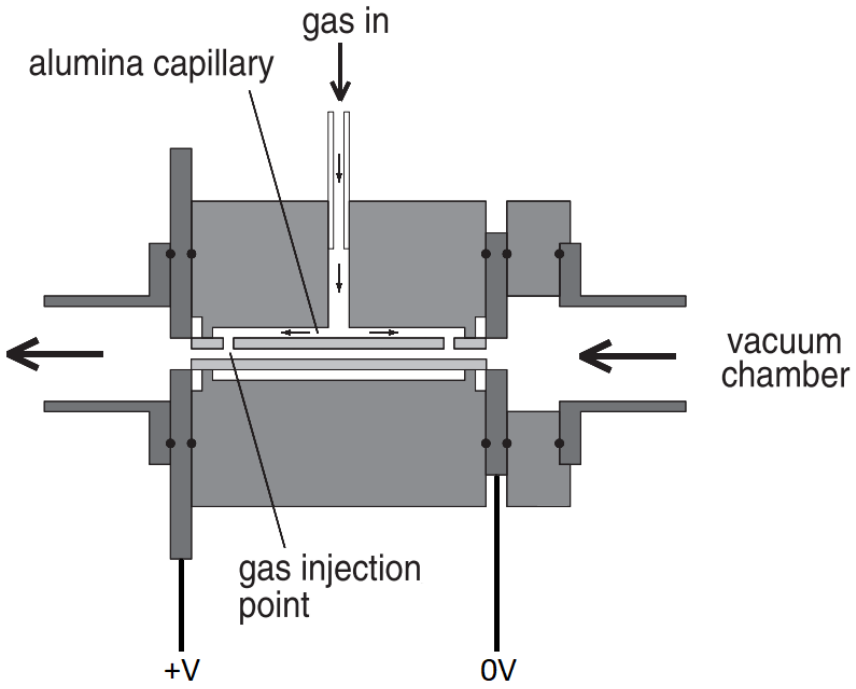

FIG. 4. Schematic diagram of the gas-filled capillary discharge waveguide. Modified from [3].

Most recently, the highest electron beam energies from a capillary discharge experiment have been 8 GeV [8]. This was achieved through several changes to previous work [14, 15]. The biggest change is the introduction of a heater pulse in addition to the capillary discharge. This pulse is a 0.4 J, 8 ns FWHM pulse that arrives between the capillary discharge and the drive pulse. The heater pulse raises the electron temperature through inverse brehmsstrahlung from 4.1 eV to 4.7 eV. This causes more hydrodynamic expansion than the original capillary discharge, increasing the density gradient, and allowing for better pulse guiding. This allowed the experimenters to lengthen the channel from 9cm to 20cm, which gives a much longer distance for electrons to accelerate, allowing for higher energies [8]. The initial gas density was decreased to $2.7 \times 10^{17} cm^{-3}$. Simulations predict increases in the electron beam energy above 10 GeV is possible by increasing in laser power and lowering plasma density while keeping the same spot size [8].

V. LASER HEATING AND OPTICAL FIELD IONIZATION

The goal of laser heating and OFI is the same as capillary discharge; to create a low density core surrounded by a higher density cladding which will help to accelerate electrons to higher energies in LWFA. However, the manner in which the plasma waveguide is formed differs from capillary discharge. In laser heating and OFI, a laser pulse is shot into a gas target, heating and ionizing the core. The hot, ionized core will start expanding into the cooler surrounding neutral gas, leaving a low density core in the middle of the plasma channel. A large density gradient is formed, producing a waveguide, and allowing for better guiding and higher fluence through the channel [6].

The idea to create electron density gradients in plasmas through laser heating was first introduced in the 1990's [19]. The first proof-of-concept laser-generated plasma waveguides relied on cylindrical shock expansion to form both the core and the cladding [19, 22]. This was done with long pulse, picosecond time scale, lasers that heat the plasma through inverse brehmsstrahlung (IB). IB heats a plasma when an electron absorbs a photon while colliding with another electron or ion. This increase in the particle energy and heats the plasma. Because this depends on electrons colliding with ions, heating is most effective with a higher number density. This creates a problem because to produce higher GeV electron beam requires lower electron densities [16], which eliminates IB as a suitable plasma channel

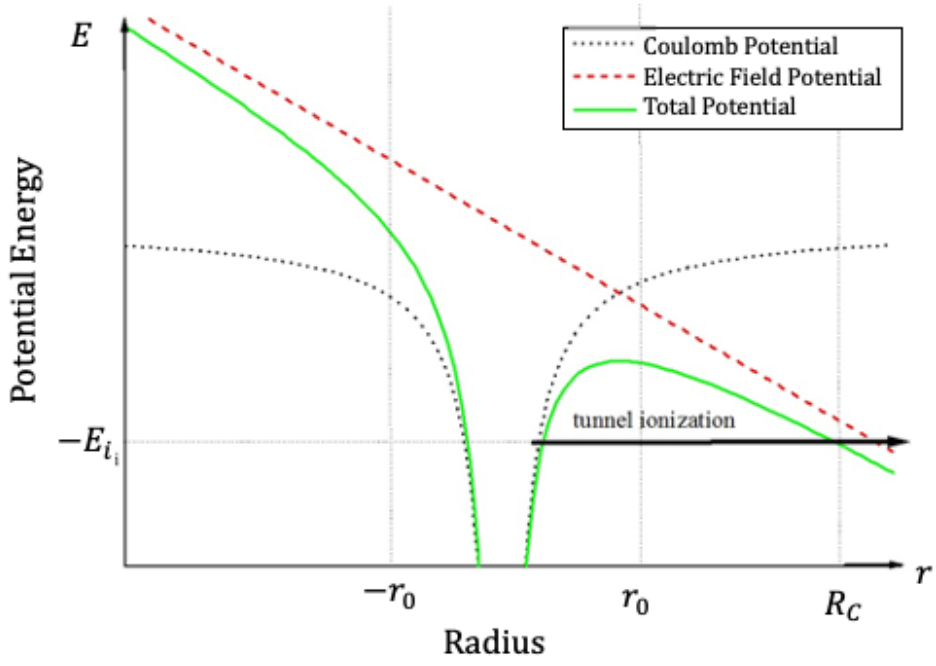

FIG. 5. The black dashed line shows the unperturbed Coulomb potential felt by an electron in an atom. The red dashed line is the potential from the intense electric field from the laser. The green dashed line is the perturbed potential the electron feels in the presence of the laser. The black arrow shows the electrons ability to tunnel out of the Coulomb potential, thus ionizing the gas. Modified from [4].

method.

A new method of heating was introduced using ultra-short (sub-picosecond) pulses to produce "above threshold" ionization heating. Above threshold ionization occurs in the presence of strong electric fields. The electric field lowers the Coulomb potential between the nucleus and an electron enough for the electron to tunnel out. The laser electric field perturbing the Coulomb potential can be seen in FIG. 5. Above threshold ionization tends to fully ionize the gas target, which leads to higher density gradients [23]. This makes it a good candidate for low density plasma waveguide generation. However, for long plasma channels, because of the low density, the heating pulse produces pressure gradients that are too weak to drive the shock that creates the core and cladding density gradient, which can lead to leakage losses [5].

More recently, experiments using Bessel pulse OFI have formed electron beams with energies up to 5 GeV [5]. Bessel pulse OFI is appealing because it has negligible leakage loss. In Bessel pulse OFI, the first pulse is a J_0 Bessel shaped pulse which completely ionizes

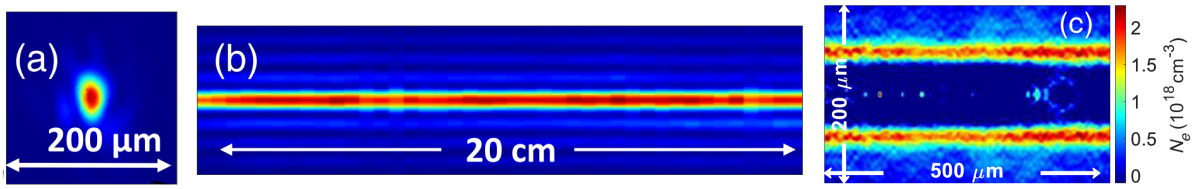

FIG. 6. (a) Focal profile of the plasma channel generating laser. (b) Longitudinal scan of the guided pulse, showing good guiding over 20cm. (c) Plasma waveguide density profile. Modified from [5].

the core of an H_2 gas target. This expands cylindrically outward into neutral H_2 gas, leaving a low density core at the middle of the target. Next, a high intensity drive pulse propagates and the leading edge of the pulse generates a plasma cladding, which forms a waveguide by OFI and confines the rest of the pulse [12]. In this experiment [5], a Bessel pulse approach was used. The plasma channel was formed by a 0.5 J, 75 fs, J_0 Bessel beam pulse. The electrons were accelerated by a 15 J, 45 fs J_0 Bessel pulse. The 20cm long plasma channel was full of hydrogen gas with an initial density of $1.3-3.2\times10^{17}\ cm^{-3}$. The plasma channel generation and drive pulse guiding can be seen in FIG. 6. This was done at the ALEPH laser at Colorado State. Electron beam energies of 0.75-6.7 GeV were measured on a magnetic spectrometer [5]. While these are currently the best electron beam energies produced from OFI, there are plans to improve energy into the >10 GeV range. The current energies were limited by pointing stability and nonuniform axial gas densities [5].

A new method of OFI channel formation was suggested where 2 Bessel beams are used to create the plasma channel [6]. The first pulse is a J_0 Bessel shaped pulse which completely ionizes the core of an H_2 gas target. This core has a radius of 3μm. This fully ionized plasma column expands cylindrical outward into neutral H_2 gas, leaving a low density core at the middle of the target. After the plasma core has expanded and cooled, a second Bessel

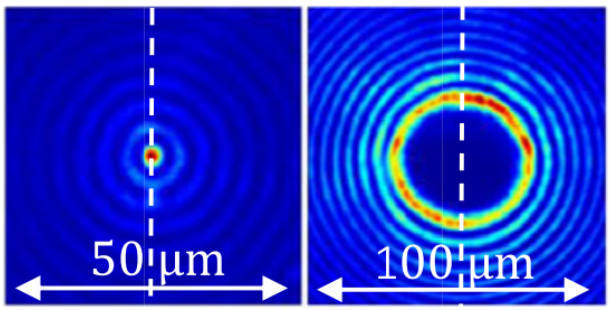

FIG. 7. Left: J_0 Bessel beam. Right: J_8 Bessel beam ring. From [6].

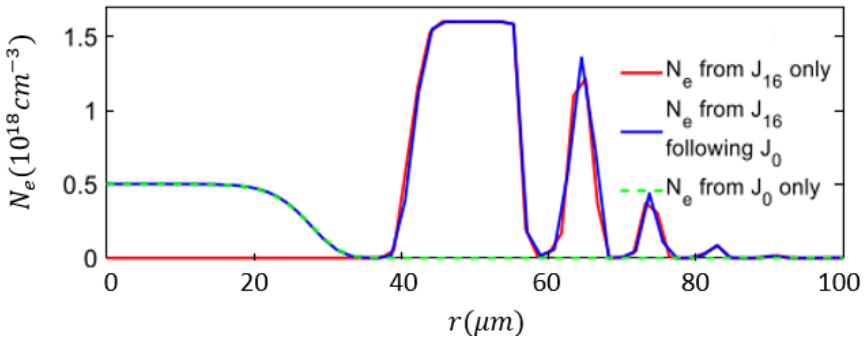

FIG. 8. Electron density produced from the J0 (green), J16 (red), and J0 and J16 pulses (blue). The core of the channel goes from 0 to 40 μm and the cladding goes from 40-60 μm. Modified from [6]

pulse follows, which is either a J_8 or J_{16} beam. This beam ionizes neutral atoms around the low density core, creating a sharp electron density gradient, and producing the cladding. No recombination occurs in the time between the first and second pulse. The second pulse has a ring like geometry which is formed by a transmissive spiral phase plate. The two Bessel pulses can be seen in FIG. 7. The introduction of the second Bessel pulse creates a higher density gradient than traditional single pulse OFI. This density gradient can be seen in FIG. 8. The increased density gradient allows for higher drive pulse power, better guiding, and better electron beam acceleration. Experimentally, the guided mode only had a 50% coupling efficiency due to poor mode matching. Simulations show that this could get close to 100%. Pointing instability plays an important role in the effectiveness of the waveguide, and is responsible for most of the shot to shot variations [6]. This method is more difficult to perform experimentally, but there are plans to implement this 2-Bessel model in a future experiment at the ALEPH laser [5]. Simulations with this plasma channel structure suggest that electron beam energies $> 10\ GeV$ can be achieved.

VI. CONCLUSION

LWFA has made many advancements since it's conception in 1979. The production of stable GeV electron beams is a great step forward towards free-electron lasers, Thomson sources, and a variety of different high energy particle colliders. Improvement of waveguiding techniques is one of the key contributors to those advancements and the most promising waveguiding techniques are capillary discharge and OFI. These waveguide methods have

shown promising results by producing up to 8 GeV electron beams with goals of going higher than that.

Moving forward, a blend of the two techniques might prove most effective, like is seen in the experiment by Gonsalves [8]. Regardless of which method is used, future work can be focused on lengthening the plasma channel to achieve higher electron beam energies, reducing pointing instability, limiting electron beam energy spread, and controlling electron injection into the LWFA.

[1] Laser wakefield acceleration (2018).

[2] E. Esarey, C. B. Schroeder, and W. P. Leemans, Physics of laser-driven plasma-based electron accelerators, Rev. Mod. Phys. **81**, 1229 (2009).

[3] D. J. Spence, A. Butler, and S. M. Hooker, First demonstration of guiding of high-intensity laser pulses in a hydrogen-filled capillary discharge waveguide, Journal of Physics B: Atomic, Molecular and Optical Physics **34**, 4103 (2001).

[4] A. Talebpour, *New advances in the interaction of a femtosecond Ti : sapphire laser with atoms and molecules*, Ph.D. thesis, Université Laval (1998).

[5] B. Miao, J. E. Shrock, L. Feder, R. C. Hollinger, J. Morrison, R. Nedbailo, A. Picksley, H. Song, S. Wang, J. J. Rocca, and H. M. Milchberg, Multi-gev electron bunches from an all-optical laser wakefield accelerator, Phys. Rev. X **12**, 031038 (2022).

[6] B. Miao, L. Feder, J. E. Shrock, A. Goffin, and H. M. Milchberg, Optical guiding in meter-scale plasma waveguides, Phys. Rev. Lett. **125**, 074801 (2020).

[7] T. Tajima and J. M. Dawson, Laser electron accelerator, Phys. Rev. Lett. **43**, 267 (1979).

[8] A. J. Gonsalves, K. Nakamura, C. Benedetti, C. V. Pieronek, S. Steinke, J. H. Bin, S. S. Bulanov, J. van Tilborg, C. G. R. Geddes, C. B. Schroeder, J. Daniels, C. Tóth, L. Obst-Huebl, R. G. W. van den Berg, G. Bagdasarov, N. Bobrova, V. Gasilov, G. Korn, P. Sasorov, W. P. Leemans, and E. Esarey, Laser-heated capillary discharge plasma waveguides for electron acceleration to 8 GeV, Physics of Plasmas **27**, 053102 (2020).

[9] W. Leemans, B. Nagler, and A. Gonsalves, Gev electron beams from a centimeter-scale accelerator, Nature Physics **2**, 696 (2006).

[10] J. Osterhoff, A. Popp, Z. Major, B. Marx, T. P. Rowlands-Rees, M. Fuchs, M. Geissler, R. Hörlein, B. Hidding, S. Becker, E. A. Peralta, U. Schramm, F. Grüner, D. Habs, F. Krausz, S. M. Hooker, and S. Karsch, Generation of stable, low-divergence electron beams by laser-wakefield acceleration in a steady-state-flow gas cell, Phys. Rev. Lett. **101**, 085002 (2008).

[11] C. Joshi, Laser-driven plasma accelerators operating in the self-guided, blowout regime, IEEE Transactions on Plasma Science **45**, 3134 (2017).

[12] L. Feder, B. Miao, J. E. Shrock, A. Goffin, and H. M. Milchberg, Self-waveguiding of relativistic laser pulses in neutral gas channels, Phys. Rev. Res. **2**, 043173 (2020).

[13] C. E. Clayton, J. E. Ralph, F. Albert, R. A. Fonseca, S. H. Glenzer, C. Joshi, W. Lu, K. A. Marsh, S. F. Martins, W. B. Mori, A. Pak, F. S. Tsung, B. B. Pollock, J. S. Ross, L. O. Silva, and D. H. Froula, Self-guided laser wakefield acceleration beyond 1 gev using ionization-induced injection, Phys. Rev. Lett. **105**, 105003 (2010).

[14] W. P. Leemans, A. J. Gonsalves, H.-S. Mao, K. Nakamura, C. Benedetti, C. B. Schroeder, C. Tóth, J. Daniels, D. E. Mittelberger, S. S. Bulanov, J.-L. Vay, C. G. R. Geddes, and E. Esarey, Multi-gev electron beams from capillary-discharge-guided subpetawatt laser pulses in the self-trapping regime, Phys. Rev. Lett. **113**, 245002 (2014).

[15] A. Gonsalves, K. Nakamura, J. Daniels, C. Benedetti, C. Schroeder, C. Toth, J. Tilborg, D. Mittelberger, S. Bulanov, J.-L. Vay, C. Geddes, E. Esarey, and W. Leemans, Generation and pointing stabilization of multi-gev electron beams from a laser plasma accelerator driven in a pre-formed plasma waveguide, Physics of Plasmas **22**, 056703 (2015).

[16] A. J. Gonsalves, K. Nakamura, J. Daniels, C. Benedetti, C. Pieronek, T. C. H. de Raadt, S. Steinke, J. H. Bin, S. S. Bulanov, J. van Tilborg, C. G. R. Geddes, C. B. Schroeder, C. Tóth, E. Esarey, K. Swanson, L. Fan-Chiang, G. Bagdasarov, N. Bobrova, V. Gasilov, G. Korn, P. Sasorov, and W. P. Leemans, Petawatt laser guiding and electron beam acceleration to 8 gev in a laser-heated capillary discharge waveguide, Phys. Rev. Lett. **122**, 084801 (2019).

[17] G. Sun, E. Ott, Y. C. Lee, and P. Guzdar, Self-focusing of short intense pulses in plasmas, The Physics of Fluids **30**, 526 (1987).

[18] J. M. Dawson, Nonlinear electron oscillations in a cold plasma, Phys. Rev. **113**, 383 (1959).

[19] C. G. Durfee and H. M. Milchberg, Light pipe for high intensity laser pulses, Phys. Rev. Lett. **71**, 2409 (1993).

[20] Y. Ehrlich, C. Cohen, A. Zigler, J. Krall, P. Sprangle, and E. Esarey, Guiding of high intensity laser pulses in straight and curved plasma channel experiments, Phys. Rev. Lett. **77**, 4186 (1996).

[21] A. Butler, D. J. Spence, and S. M. Hooker, Guiding of high-intensity laser pulses with a hydrogen-filled capillary discharge waveguide, Phys. Rev. Lett. **89**, 185003 (2002).

[22] C. G. Durfee, J. Lynch, and H. M. Milchberg, Development of a plasma waveguide for high-intensity laser pulses, Phys. Rev. E **51**, 2368 (1995).

[23] N. Lemos, T. Grismayer, L. Cardoso, G. Figueira, R. Issac, D. A. Jaroszynski, and J. M. Dias, Plasma expansion into a waveguide created by a linearly polarized femtosec-

ond laser pulse, Physics of Plasmas **20**, 063102 (2013), https://pubs.aip.org/aip/pop/article-pdf/doi/10.1063/1.4810797/16650867/063102_1_online.pdf.